th line to the $(f+1)-i+1$ -th line of A_1, which is defined as A_{1i}. e_i' is a column vector whose value is all 0 except for the i-th point. Then according to the literature [4] can get:

$$\mathbf{y}_{1i} = \mathrm{A}_{1i}\,\Phi^{i-1}\,\mathrm{p} + \frac{K}{MN}\sigma_n^2\,\mathrm{e}_i' \tag{24}$$

Therefore, you can get:

$$\begin{aligned} \boldsymbol{R}_i &\triangleq E\{\boldsymbol{y}_{1i}\boldsymbol{y}_{1i}^{\mathrm{H}}\} = \boldsymbol{A}_{11}\boldsymbol{\Phi}^{i-1}\mathrm{p}\,\mathrm{p}^{\mathrm{H}}(\boldsymbol{\Phi}^{i-1})^{\mathrm{H}}\boldsymbol{A}_{11}^{\mathrm{H}} \\ &+\frac{K^2}{M^2N^2}\sigma_n^2\,\mathrm{e}_i'\,\mathrm{e}_i'^{\mathrm{H}} + \frac{K}{MN}\boldsymbol{A}_{11}\boldsymbol{\Phi}^{i-1}\mathrm{p}\,\mathrm{e}_i'^{\mathrm{H}} \\ &+\frac{K}{MN}\sigma_n^2\,\mathrm{e}_i'\,\mathrm{p}^{\mathrm{H}}(\boldsymbol{\Phi}^{i-1})^{\mathrm{H}}\boldsymbol{A}_{11}^{\mathrm{H}} \end{aligned} \tag{25}$$

For averaging different i, the covariance matrix after spatial smoothing:

$$\boldsymbol{R}_{ss} = \frac{1}{(f+1)/2}\sum_{i=1}^{(f+1)/2}\boldsymbol{R}_i \tag{26}$$

It can be applied to DOA estimation.

4.3 Performance analysis

The example given is shown in Figure 1. The transmitting end has three array elements in the horizontal direction, $N=20$ in the vertical direction (only three are drawn in the figure), and four array elements in the receiving end. Because of the symmetry of the position of the array element, we only draw a non-negative part in the difference coarray. According to the foregoing, since the horizontal aperture of the array of the difference of the array is 7, the expansion ratio of the array element at the receiving end is $S=7$. Therefore, the difference coarray formed by the virtual array is a "hole-free" two-dimensional array.

The two-dimensional hybrid phased-MIMO radar is similar to our proposed hybrid phased-MIMO radar. The difference is that the nested array arrangement in the horizontal direction of the transceiver becomes a coprime arrangement. In order to make the comparison clearer, we chose to use the coprime array with closed expression proposed in [11]. In the lateral direction, the coprime arrays consists of a pair of ULAs having $M_c\cdot\lambda/2$ and $N_c\cdot\lambda/2$ cell spacings, where λ is the signal wavelength and M_c and P_c are the coprime integers.

At this time, the relationship between the number of elements in the one-dimensional coprime arrays obeys the following relationship: $2M_c+P_c-1=Q$, and requires M_c 、 P_c to be coprime, and the values of $2M_c-1$ and P_c should be similar, so as to ensure the maximum DOF of the coprime array. According to [11], the maximum DOF of the coprime arrays, $DOF_{c\max}=\{(7M_c-3)P_c+M_c\}\cdot N$. Wherein, M_c, P_c, and DOF_c respectively represent the horizontal array element number of the transmitting end of the coprime array, the number of receiving end array elements, and the representative nested array corresponding to DOF, M_n, P_n and DOF_n.

In order to satisfy the condition of coprime, the values of $2M_c-1$ and P_c are not approximately equal. In order to compare the best performance of the coprime array and the nested array, we construct a Q value that satisfies $2M_c-1=P_c$ and then compare them:

Table 1 DOF of discontinuous Q value

Q	*10*	*18*	*26*	*34*	*42*
M_c	3	5	7	9	11
P_c	5	9	13	17	21
DOF_c	93N	293 N	605 N	1029 N	1565 N
M_n	5	9	13	17	21
P_n	5	9	13	17	21
DOF_n	289 N	2401 N	9409 N	2592 1N	5808 1N

It can be seen from Table 1 that the DOF of the coprime hybrid phased-MIMO radar still lags behind the nested hybrid phased-MIMO radar, despite the optimal arrangement of the coprime array. This is because $DOF_{c\max}$ can only implement the DOF of $O(Q^2)\cdot N$, and the nested hybrid phased-MIMO radar can achieve $O(Q^4)\cdot N$.

5 Simulation Results

We use computer simulation to verify the performance of traditional, coprime and nested hybrid phased-MIMO radars.

Consider an example, shown in Figure 1, where $M_o=3$, $P_o=4$, $M_c=3$, $P_c=2$, $M_n=3$, $P_n=4$, take $N=20$, and detect 36 incoherent targets in space, their coordinates are evenly spaced at azimuth 20-70 degrees, pitch angle In the square area of 20-70 degrees. 2-D MUSIC spectra were estimated for these targets using a hybrid phased-MIMO radar and a nested hybrid phased-MIMO radar, respectively. The results are shown in Figure 2:

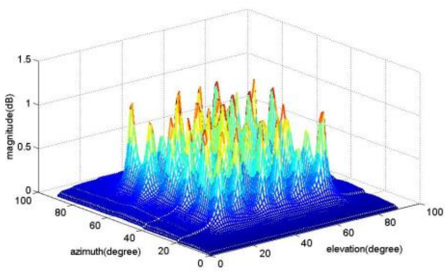

(a) MUSIC spectrum of traditional two-dimensional hybrid phased-MIMO radar

 https://doi.org/10.1051/matecconf/201823202052

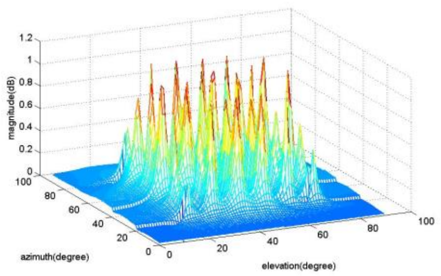

（b）MUSIC spectrum of coprime two-dimensional hybrid phased-MIMO radar

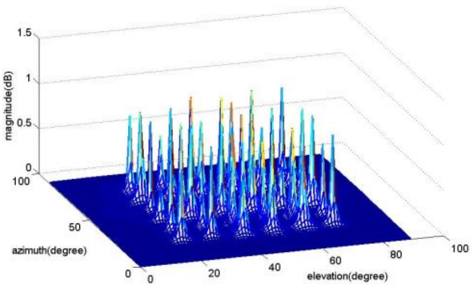

（c） MUSIC spectrum of nested two-dimensional hybrid phased-MIMO radar

Figure 2 Three types two-dimensional hybrid phased-MIMO radar MUSIC spectrum

It can be seen from the three-dimensional MUSIC spectrum of Fig. 2 that the spectral peaks of the conventional two-dimensional hybrid phased-MIMO radar are very unclear, and some degree of aliasing and distortion occur, and the effect of detecting targets is poor; Coprime hybrid phased-MIMO radar has a better MUSIC peak, but a few estimated peaks deviate from the correct position; and the nested two-dimensional hybrid phased-MIMO radar MUSIC peak is clear and complete, accurately and completely estimated 36 targets.

In order to show the accuracy of the estimation more clearly, we compare the root-mean-square error (RMSE) of the three DOA estimates. For these 36 sources, the Monte Carlo number is 100. As shown in Figure 3:

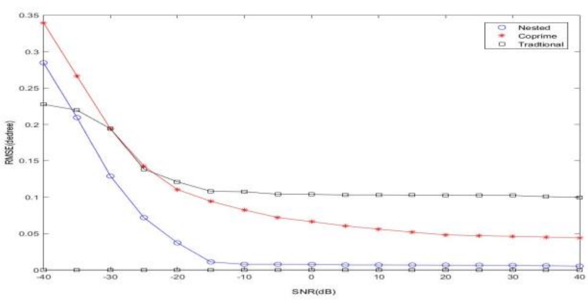

Figure 3 RMSE comparison chart

It can be seen that, except in the environment with extremely low signal-to-noise ratio, the mean square error of the traditional hybrid phased-MIMO radar is slightly smaller than that of the coprime and nested hybrid phased-MIMO radar. As the signal-to-noise ratio increases, the RMSE of this nested two-dimensional hybrid phased-MIMO radar is significantly lower than that of the two-dimensional hybrid phased-MIMO radar. This is because the difference coarray of "hole-frees" brings great expansion to the virtual aperture, so that the nested two-dimensional hybrid phased-MIMO array can be compared with the traditional and the coprime array, and the number of elements is the same. This nested structure performs less well than the traditional hybrid phased-MIMO radar in low SNR environments, but performs well under high SNR conditions. In this case, there is a more accurate DOA estimation accuracy for the same spatial target. Therefore, it can be considered that the nested two-dimensional hybrid phased-MIMO radar has better DOA estimation performance in a high SNR environment.

6 Conclusion

In this paper, a two-dimensional hybrid phased-MIMO radar based on nested array is constructed by using the properties of nested arrays. Furthermore, the array manifold is derived, as well as the position of the array element and the closed expression of the DOF. More importantly, the difference coarray of nested arrays is "hole-free", which maximizes the use of difference coarrays to extend array aperture and DOF compared to traditional and complementary two-dimensional hybrid phased-MIMO radars. A larger aperture and DOF can be obtained given the number of elements, and the DOA estimates better performance.

7 Acknowledgements

This work was supported by Project Supported by the National Natural Science Fund of China (61671465).

References

1. A. Hassanien, S. A. Vorobyov. Phased-MIMO radar: A tradeoff between phased-array and MIMO radars[J]. IEEE Trans. on Signal Processing, 2010, **58**(6): 3137-3151.
2. A. Hassanien, S. A. Vorobyov. Y. S. Yoon, et al. *Two-stage based design for phased-MIMO radar with improved coherent transmit processing gain*[C] // Signal Processing Advances in Wireless Communications (SPAWC), 2014 IEEE 15th International Workshop on. IEEE, Toronto, ON, Canada: IEEE Press. 2014: 45-49.
3. A. Deligiannis, S. Lambotharan, J. A. Chambers. *Beamforming for fully-overlapped two-dimensional phased-MIMO radar*[C]. // IEEE Radar Conference (RadarCon), Arlington, VA, USA: IEEE Press. 2015:0599-0604.
4. C. Chen, P. P. *Vaidyanathan. Minimum redundancy MIMO radars*[C] // IEEE International Symposium on Circuits and Systems. Seattle, WA, USA: IEEE Press. 2008: 45-48.
5. J. Li, D. Jiang, X. Zhang. DOA estimation based on combined unitary ESPRIT for coprime MIMO

radar[J]. IEEE Communications Letters, 2017, **21**(1): 96-99.
6. P. Piya, P. P. Vaidyanathan. Nested array: a novel approach to array processing with enhanced degrees of freedom[J]. IEEE Trans. on Signal Processing, 2010, **58**(8):4167-4181.
7. L. Mao, H. Li, Q. Zhang. Transmit Subaperturing for MIMO Radars with Nested Arrays[J]. Signal Processing, 2017, 134: 244-248.
8. M. Yang, L. Sun, X. Yuan, et al. A New Nested MIMO Array With Increased Degrees of Freedom and Hole-Free Difference Coarray[J]. IEEE Signal Processing Letters, 2018, **25**(1): 40-44.
9. C. Zhu, H. Chen, Shao H. Joint phased-MIMO and nested-array beamforming for increased degrees-of-freedom[J]. International Journal of Antennas and Propagation, 2015: 1-11.
10. S. LIU, B. WANG, X. LI, et al. Design of receiving array of two-dimensional nested hybrid Phasd-MIMO radar[J]. Acta Aeronautica et Astronautica Sinic. 2018, **39**(4): 173-181.
11. Y. Gu, C. Zhou, N. A. Goodman, et al. *Coprime array adaptive beamforming based on compressive sensing virtual array signal*[C] // 2016 IEEE International Conference on Acoustics, Speech and Signal Processing (ICASSP), Shanghai, China: IEEE Press. 2016: 2981-2985.